NANOPHOTONIC SILICON ELECTRO-OPTIC SWITCH

by

Deepak Venkatesh Simili

Submitted in partial fulfillment of the requirements

for the degree of Master of Applied Science

at

Dalhousie University

Halifax, Nova Scotia

August 2012

DALHOUSIE UNIVERSITY

DEPARTMENT OF ELECTRICAL AND COMPUTER ENGINEERING

The undersigned hereby certify that they have read and recommend to the Faculty of Graduate Studies for acceptance a thesis entitled "Nanophotonic Silicon Electro-Optic Switch" by Deepak Venkatesh Simili in partial fulfilment of the requirements for the degree of Master of Applied Science.

Dated: 27th August 2012

Supervisor: —————————————————

Dr. Michael Cada

Readers: —————————————————

Dr. Zhizhang Chen

—————————————————

Dr. Srinivas Sampalli

DALHOUSIE UNIVERSITY

DATE: 27th August 2012

AUTHOR: Deepak Venkatesh Simili

TITLE: Nanophotonic Silicon Electro-Optic Switch

DEPARTMENT OR SCHOOL: Department of Electrical and Computer Engineering

DEGREE: M.A.Sc.   CONVOCATION: May   YEAR: 2013

Permission is herewith granted to Dalhousie University to circulate and to have copied for non-commercial purposes, at its discretion, the above title upon the request of individuals or institutions. I understand that my thesis will be electronically available to the public.

The author reserves other publication rights, and neither the thesis nor extensive extracts from it may be printed or otherwise reproduced without the author's written permission.

The author attests that permission has been obtained for the use of any copyrighted material appearing in the thesis (other than the brief excerpts requiring only proper acknowledgement in scholarly writing), and that all such use is clearly acknowledged.

_____
Signature of Author

Dedication

This thesis is dedicated to my parents, S.V Venkatesh and Jayashree Venkatesh, as well as to my brother Dwarakanath S.V, for their continued encouragement, support and best wishes.

Table of Contents

LIST OF TABLES

LIST OF FIGURES

ABSTRACT

The design procedure for ultrafast silicon electro-optic switches using photonic crystals in order optimize the operation of the electro-optic switch is presented. The material medium selected for propagation of the optical signal through the switch is silicon nanocrystals in silica. A patterned slot waveguide with one-dimensional photonic crystals is proposed as the preferred slow light waveguide to be used in the design of the electro-optic switch. The ultrafast quadratic electro-optic Kerr effect is the physical effect utilized, and its analysis for slot waveguides is discussed. The optical structure analysis of the electro-optic switch using a ring resonator is presented and it is shown that the use of a slow light waveguide in the ring resonator can reduce the required externally applied electric field and the radius of the ring resonator.

LIST OF ABBREVIATIONS AND SYMBOLS USED

$\chi^{(3)}$ Third order nonlinear susceptibility of the material(m^2/V^2)

n_2 Kerr coefficient of the material (m^2/W)

β_2 Nonlinear absorption (m/GW)

n_L Linear refractive index of the material

n_s Refractive index of the low index medium in the slot waveguide

n_H Refractive index of the low index medium in the slot waveguide

w_s Width of the slot region (m)

w_h Width of the high refractive index medium in the slot waveguide (m)

n_C Refractive index of the cladding surrounding the slot waveguide

E_S Component of the electric field in the low refractive index region of the slot waveguide (V/m)

E_H Component of electric field in the low refractive index region of the slot waveguide (V/m)

a Periodic spacing distance between two layers of the same material in in a multilayer film (m)

ω Angular frequency of the optical mode (*rad. /s*)

k Angular wave number of the optical mode in the medium (m^{-1})

c Phase velocity of the optical mode in the medium (*m/s*)

ε Electric permittivity of the medium (*F/m*)

n Optical mode number

L Length of the waveguide required to induce a relative phase shift $\Delta\phi$ in the optical signal (m)

$\Delta\phi$ Induced phase shift in the optical signal as it propagates through a waveguide. (*radians*)

λ_{air} Wavelength of the optical signal in air. (m)

Δn Refractive index change induced in the material.

v_g Group velocity of the optical signal. (*m/s*)

$\Delta\omega(k)$ Shift in the photonic band mode for a fixed angular wave number k (*rad. /s*)

σ Fraction of the electric field energy inside the region where Δn is applied

$\Delta k(\omega)$ Change in the wave number of optical signal. (m^{-1})

k_0 Wavenumber of the optical signal in vacuum (m^{-1})

Λ Separation between the point defects in the photonic crystal waveguide (*m*)

Δn_{eff} Effective modal index of the material inside the waveguide

Δn_{mat} Material change in refractive index

n_{eff} Effective refractive index of the material inside a waveguide

β Propagation constant of the waveguide. (m^{-1})

k_{air} Wavenumber of the optical mode in air (m^{-1})

c_0 Phase velocity of the optical mode in air (*m/s*)

S Slowdown factor of the medium

v_ϕ Phase velocity of the optical mode in the medium. (*m/s*)

Δn_{mat} Material change in refractive index

h Thickness of the silicon slabs that comprise the slot waveguide (*m*)

E d.c electric field (*V/m*)

$n(E)$ Refractive index as a function of the applied electric field

$a_{1,2}$ Taylor series coeffecients

$P^{(n)}(t)$ nth order polarization density vector ogf the medium (C/m^2)

$E_j(\omega)$ jth electric field due to the optical signal of frequency ω (*V/m*)

E_{ext} Externally applied electric field (*V/m*)

ε_0 Electric permittivity of free space (*F/m*)

n_{Si} Refractive index of silicon material

n_{Si-nc} Refractive index of silicon nanocrystals material

n_{SiO_2} Refractive index of silica

E_s Electric field within the slot region(*V/m*)

V_{ext} Applied external constant voltage (V)

t_n Thickness of the nth layer in the slot waveguide structure (m)

T Transmission through the straight waveguide in a ring resonator

a_R Attenuation coefficient in the ring waveguide

t Straight through coefficient

α Amplitude attenuation coefficient to account for losses due to bending and scattering in the ring waveguide (m^{-1})

θ Phase shift experienced by the optical signal after it completes one round trip of the ring waveguide (*radians*)

$\Delta\lambda_{res}$ Change in the resonant wavelength of the ring resonator (m)

R Radius of the ring resonator (m)

E_{old} Applied d.c electric field for a ring resonator with a conventional waveguide (*V/m*)

E_{new} Applied d.c electric field for a ring resonator with a slow light waveguide (*V/m*)

Si   Silicon

Si-nc   Silicon nanocrystals

SiO_2 Silica

GaAs   Gallium Arsenide

GaAlAs   Gallium Aluminum Arsenide

FSR   Free Spectral range

1D PhoCSloW   One-dimensional photonic crystals embedded in a slot waveguide

LPCVD   Low-pressure chemical vapour deposition

PECVD   Plasma-enhanced chemical vapour deposition

FDTD   Finite Difference Time Domain

CROW   Coupled Resonator Oscillator Waveguide

PC   Photonic Crystals

CCW   Coupled Cavity Waveguide

TPA   Two Photon Absorption

ACKNOWLEDGEMENTS

CHAPTER 1   INTRODUCTION

1.1 Overview

Photonics is a scientific discipline that deals with the interaction between fundamental particles of light and matter, which are photons and electrons respectively. Photonics has basically developed from the field of optics, which involves the science of generation, transmission and detection of light. As the ties between optics and electronics began to grow due to the increasing usage of semiconductors in optical systems, the term photonics was coined as an analogy to the term electronics. 'Electronics' involves the control of the flow of electrons and similarly photonics refers to the control of the flow of photons [1].

Silicon is one of the most widely used semiconductors in the electronics industry and it has the potential to be widely used for photonics. Analysis of the behaviour of silicon for physical effects such as the electro-optic effect were first carried out by R.A. Soref and B R. Benett in the year 1987 [2] . Such an analysis is a requirement for the application of silicon for photonic devices. In the area of Integrated Optics — where different optical devices such as modulators, switches, etc. are combined on a single chip — silicon photonics would play a key role. The motivating factors for the development of silicon photonics are:

1) Compatibility with mature and well developed silicon integrated circuit manufacturing. Thus, there is potential for low-cost photonics for mass market applications using silicon

2) Fabrication of nanometer scale photonic devices. This would result in a strong optical confinement in the photonic device resulting in nonlinear effects (for example, the Kerr effect)

3) Excellent material parameters for photonic devices exhibited by silicon. Silicon has a greater third order nonlinear susceptibility than silica glass and has a low

loss window from 1-7 micrometres [3], which includes the optical communication wavelength of 1.55 micrometers.

To enhance the photonic device performance, the use of nanophotonic structures looks promising. Nanophotonics deal with light and matter interaction at the nanometer scale [4]. When confined to the nanometer scale, light and matter begin to show new physical properties [4, 5] that could be useful for novel photonic devices such as electro-optic switches.

Electro-optics is a branch of optics that involves an applied external electric field through a voltage source on a medium and an optical signal propagating through the medium. The underlying effect or phenomenon that is used in electro-optics is the electro-optic effect. The electro-optic effect, as defined in [1], "is the change in the refractive index of the medium resulting from the application of an electric field (d.c or low frequency)". This fundamental effect is utilized in implementing an electro-optic switch. Figure 1.1 describes the electro-optic effect wherein the material property (i.e. refractive index) is changed by the application of a steady electric field, which results in a change in the phase of the optical signal coming out of the material.
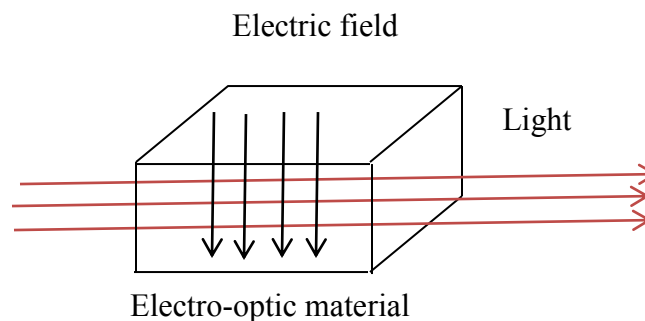

Figure 1.1 Control of light by the applied electric field
through the electro-optic material [1]

1.2 Motivation and Thesis Objective

The main motivation for our research project is to design an ultrafast silicon electro-optic switch with speeds of the order of 100 GHz. Such high speed devices would be useful in optical communication networks in order to process large spectral bandwidth optical signals. Transmission bandwidths of up to 30 GHz have been achieved using a silicon electro-optic modulator in which the free carrier plasma dispersion effect is utilized to induce a change in the refractive index of the medium [6]. The drawback of the free carrier effects is that it offers low switching speeds due to relatively long (around 1 ns) free carrier recombination [7]. Another physical effect that has commonly been used for electro-optic devices is the linear electro-optic effect. This effect is not existent in silicon. Materials that possess strong second order nonlinearity such as lithium niobate and III/V semiconductors have been used in such cases. Due to integration and technological compatibility issues, devices based on the linear electro-optic effect have not been widely used [8]. Other driving factors include polarization independence in the electro-optic switch, thereby eliminating losses related to polarization. Scalability and integration with other optical devices are also desired which would require reduction in the drive voltage and size of the electro-optic device.

An alternative approach is to utilize the third order nonlinearity of silicon for the switching operation. The third order nonlinearity as a material property has traditionally been used for all-optical effects such as self-phase modulation, four wave mixing and others. Instead of using the all-optical effects, it has been shown in [8] that the quadratic electro-optic Kerr effect can be utilized to achieve ultrafast switching in a silicon-based electro-optic device with speeds of the order of 100 GHz.

Nanophotonic structures such as silicon nanocrystals, slot waveguides and photonic crystals have unique properties such as high material nonlinearity, strong confinement and enhanced phase sensitivity [9,10,11] respectively. The objective of this thesis is to utilize the above mentioned advantages of nanophotonic structures in order to optimize the operation of a silicon electro-optic switch.

1.3 Thesis Outline

The outline of my thesis is as follows. Chapter 2 describes Nanophotonic structures and their unique properties. Chapter 3 explains the quadratic electro-optic Kerr effect, which is used in the operation of the switch. Chapter 4 provides an optical structure analysis and explains the advantage of using a Nanophotonic structure in the design of the electro-optic switch. Chapter 5 summarizes the conclusions drawn from my research project and lists future steps to undertake to proceed further to my research goal.

CHAPTER 2   NANOPHOTONIC STRUCTURES

Progress in science has been driven by observing phenomena that are not directly observable to the human eye. One example is Galileo Galilei using a telescope to observe craters and mountains on the Earth's moon for the first time. With this observation, the field of astronomy took shape. Similarly, the field of biology developed when microscopic organisms such as bacteria and protozoa were observed using an optical microscope [5]. In modern science, more and more findings are withheld from our senses, for example, the study of nanometer-sized particles, sub-atomic particles and biological samples. Therefore, the development of correct optical techniques and optical instrumentation is vital in the study of the areas mentioned above.

Presently there is a strong push for the development of nanoscience and nanotechnology. This drive is mainly due to the miniaturization and integration of electronic circuits in the computer and communication industry. The possibility of exploiting new physical effects that occur at the nanometer scale for technological applications is also one of the driving forces for the development of nanoscience. The progress in nanosceince and technology has been brought about by the ability to measure, fabricate and modify structures at the nanometer scale through sophisticated optical techniques and instruments [5].

In nature, too, there are examples of nanostructures that produce unique optical effects. Examples are the diffractive structures used by butterflies and peacocks to produce attractive colours and nanoscale structures used as antireflective coatings in the retina of insects [5]. In recent years, humans have developed nanophotonic structures — photonic crystals, nanoparticles and metal nanostructures, to name a few — for technological applications.

The novel part of our research project is the application of the nanophotonic structure, namely photonic crystals for an electro-optic switch. The purpose of this chapter is to intoduce the reader to the field of nanophotonics and the use of nanophotonic structures. Section 2.1 provides an overview of the field of nanophotonics. Sections 2.2, 2.3 and 2.4

explain specific nanophotonic structures used in this project, namely nanocrystals, slot waveguides and photonic crystals.

2.1 Overview of Nanophotonics

Nanophotonics is an interesting and emerging field that deals with the theoretical study and applications of light and matter interaction at the nanometer scale [4]. The broad categories of nanophotonics is shown in Figure 2.1 below.
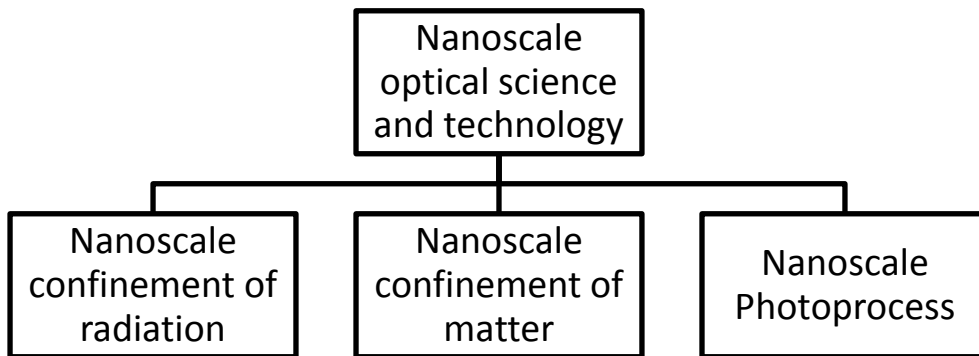
Figure 2.1 Categories in the field of Nanophotonics [4]

One way to achieve light and matter interaction on the nanometer scale is by confining light or electromagnetic wave to a space of nanometer scale dimensions. Here, the light waves, which have a wavelength range between 400 to 700 nm, are confined to geometries that have subwavelength dimensions. Examples of such cases are light emerging from a subwavelength aperture and the exponentially decaying evenescent waves that exist in the region outside the vicinity (or subwavelength distance) of the waveguide. The unique physical effect of confinement is the generation of near field optical waves, which are optical waves in the vicinity of the subwavelength size aperture. An example of this near field wave is the evanescent wave that is used for light propagation in slot waveguides[10]. Another example of the utilization of near field

waves is in near field scanning optical microscopes. In this case, the samples are sensed using near field waves, resulting in a resolution greater than the diffraction limit [4].

In the nanoscale confinement of matter, a material such as, for example, silicon is transformed from its bulk form to particles called silicon nanocystals, which have diameters of the order of 1 to 10 nm. Another way to bring about nanoscale confinement of matter is to develop a structure wherein there is periodic change in the dielectric material, with repetition distance being of the order of nanometers. Such structures are called photonic crystals and will be explained later in the chapter. The purpose of the nanoscale confinement of matter is to use the enhanced material nonlinear properties due to quantum confinement[9,12] for applications such as switching. Another driving factor is to utilize unique physical effects such as slowing down the group velocity of the optical signal using photonic crystals [11, 13].

The nanoscale photoprocess deals with the nanometer confinement of photoprocesses or a light-induced process. This technique can be used for the fabrication of photonic structures in the nanoscale domain [4].

A brief explanation about the important branches of nanophotonics has been presented in this section, thus providing an overview of the field. The following sections aim to explain in detail specific examples of nanophotonic structures that are important for this thesis.

2.2 Nanocrystals

For a silicon-based electro-optic device, it is desired that the material possess large nonlinear material properties — i.e., third order nonlinear susceptibility ($\chi^{(3)}$) — and that the Kerr coefficient (n_2) . For bulk silicon and silica, $\chi^{(3)}$ is very weak (3 x 10^{-19} m^2/V^2 for bulk silicon and 2.2 x 10^{-18} m^2/V^2 for silica at wavelength of 1550 nm [14]) to be useful for an electro-optic switch.

It has been shown that reducing the size of a material to the order of nanometers drastically enhances third order nonlinear susceptibility of the material due to quantum

confinement effects [15]. The new structure of the material is called a nanocrystal, which has a diameters of approximately 1nm [16].

Apart from having large material nonlinearities, it is highly desired that the material be able to be mass-manufactured. A material that satisfies both these criteria is silicon nanocrystals embedded in silica ($Si - nc/SiO_2$), which has been used in the design of an ultrafast all-optical switch [7]. Secondly, silicon nanocrystals in silica can be mass-manufactured through standard fabrication methods such as low-pressure chemical vapour deposition (LPCVD) or plasma-enhanced chemical vapour deposition (PECVD) as noted in [7]. From [14,7], the following comparison between important nonlinear material properties at wavelength of 1.55 micrometers is presented in Table 1.

Table 1 Material Properties

Material	Third order nonlinear susceptibility $(\chi^{(3)})$ (m^2/V^2)	Kerr Coefficient $(n_2)(m^2/W)$	Absorptio-n (β_2) (m/GW)	Linear refracti--ve index (n_L)
Silica glass	2.2×10^{-22}	3×10^{-20}	negligible	1.45
Silicon	3×10^{-19}	7×10^{-18}	0.009	3.502
Silicon nanocrystals in silica	2×10^{-18}	2×10^{-16}	0.7	1.7
Silicon nanocrystals embedded in silica (LPCVD) $(Si - nc/SiO_2)$	Not available	2×10^{-16}	0.5	Not available
Silicon nanocrystals embedded in silica (PECVD)	Not available	4×10^{-17}	0.05	Not available

From Table 1, one can observe that silicon nanocrystals embedded in silica provide at least one order of magnitude improvement in the material nonlinear parameters as compared to bulk silicon and silica glass. This suggests that the material silicon nanocrystals in silica could be useful to implement a silicon-based electro-optic switch.

The Nanophotonic structure of nanocrystals has been introduced in this section. The literature related to silicon nanocrystals has been reviewed. A comparison of important nonlinear material properties has been presented, which is useful in selecting a material for the design of a silicon-based electro-optic switch. The linear refractive index of silicon nanocrystals is around that of silica (1.45) for low silicon content [7]. As a result, this material cannot be used as the inner dielectric in conventional waveguides to confine light through total internal reflection. In order to overcome this problem, a special type of waveguide called the slot waveguide is used. The slot waveguide is also a nanophotonic structure and will be the focus of the next section.

2.3 Slot waveguides

In conventional optical systems, free space optical transmission is employed where the optical beam is transported between different locations through mirrors, lenses and prisms. In such a type of optical transmission, the optical beam experiences losses in the form of scattering and obstruction from various objects. To overcome these issues, the technology of guided wave optics has been developed. In guided wave optics, light is transmitted through enclosed dielectrics and can be used for long-distance light transmission. Other applications of guidedwave optics are in establishing secure communication, fabrication of miniaturized optical and optoelectronic devices requiring confinement of light [1].

An optical waveguide is an enclosed light transmission medium. There are three types of optical waveguide structures namely slab, strip and fiber, which are shown in Figure 2.2.

a) Slab waveguide   b) Strip waveguide

c) Optical fiber
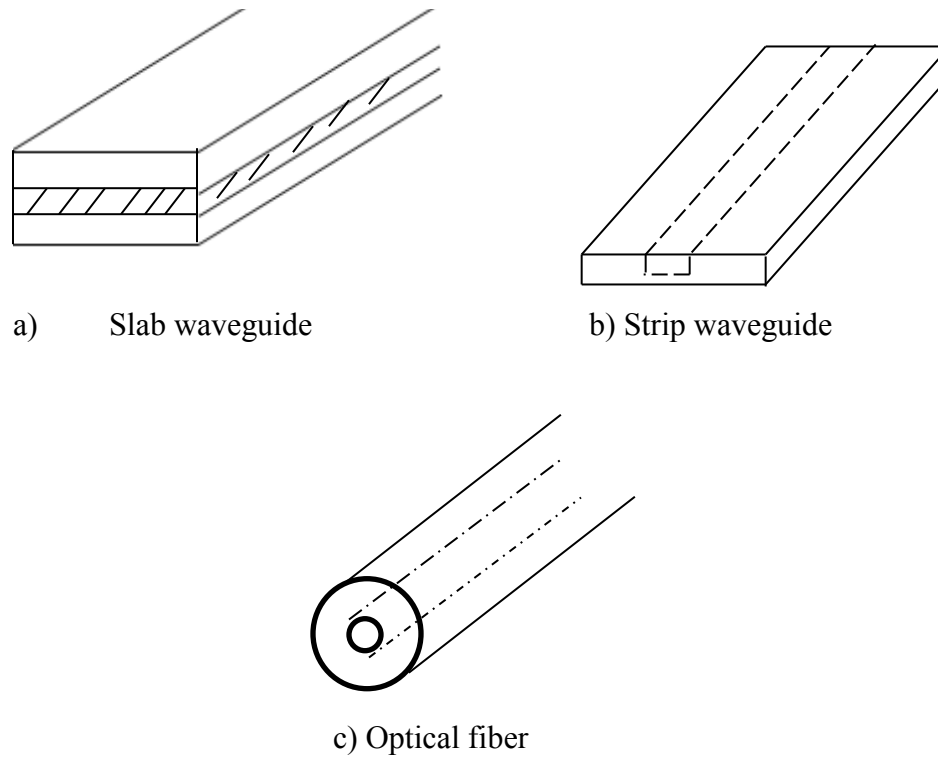
Figure 2.2 Optical Waveguides [1]

Each type of optical waveguide has an inner dielectric material of higher refractive index (shown in Figure 2.2 as a region within the shaded and dotted lines) and an outer dielectric medium of lower refractive index. The principle of light transmission through the optical waveguide is total internal reflection, so the transmission of the optical signal is basically in the medium of high refractive index. Therefore, one has to rely on the optical properties of the high-refractive index material when guiding light through an optical waveguide.

Instead of relying on the optical properties of the high-refractive index medium, one can use a slot waveguide, where confinement of an optical signal is achieved in the low refractive index medium [10,17] and therefore the optical properties of the low refractive index medium is utilized.

The typical structure of a slot waveguide is shown in Figure 2.3. In the figure n_s is the low refractive index material of width w_s present in between rectangular shaped regions having a higher refractive index of n_H and width w_h. The narrow space between the high refractive index materials is called the slot. The whole structure is present inside a low refractive index material (n_C) to ensure lateral and verticle confinment of the optical signal.

Figure 2.3 a) Schematic of slot waveguide structure [10]

Figure 2.4 Transverse electric field pattern for a quasi-TE mode in a SOI based slot waveguide [17]

It has been shown in [10,17] that the optical field can be confined and enhanced in the low refractive index material even when light is guided by total internal reflection .

The principle of operation in a slot waveguide is based on Maxwell's boundary condition in a homogeneous medium, which states that the normal components of the electric flux density must be continous.
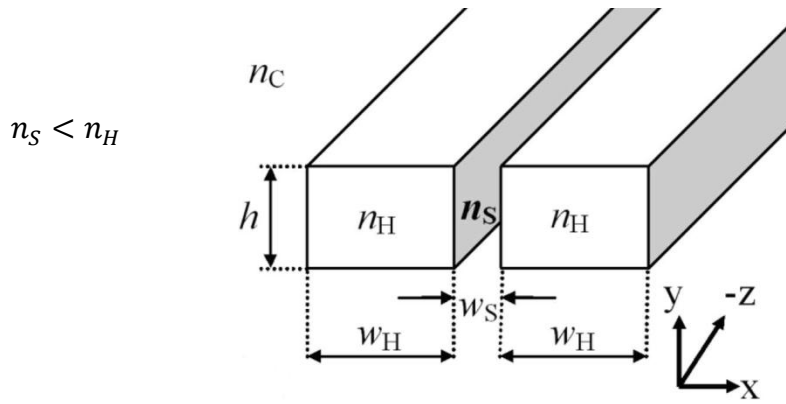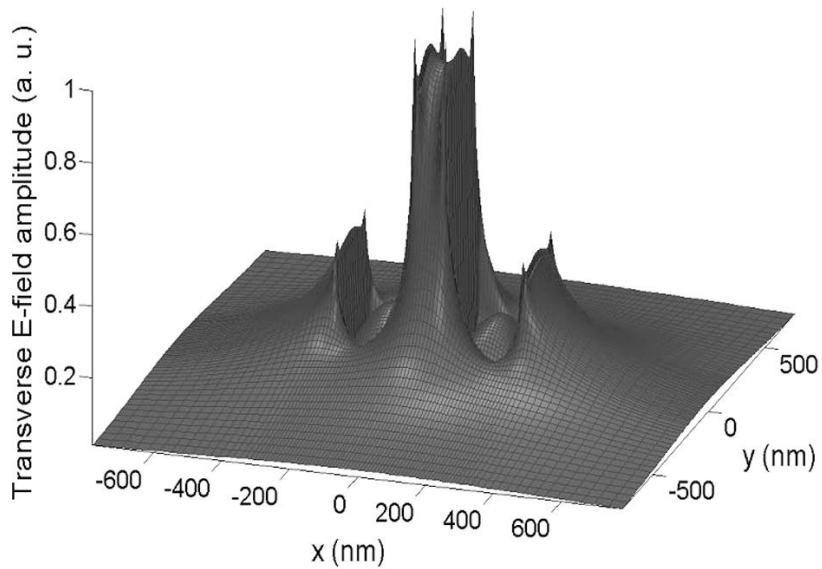
Applying the boundary condition at the interface between the high and low refractive index materials, we get:

$$\frac{E_S}{E_H} = \left(\frac{n_H^2}{n_S^2}\right)$$ (2.1)

Where E_S is the component of the electric field in the low refractive index medium that is normal to the interface between the two dielectrics, E_H is the normal component of the electric field in the high refractive index region, n_S is the refractive index of the medium inside the slot region and n_H is the refractive index of the recetangular slabs, which sandwich the slot region. From eq. (2.1) we can conclude that the normal component of the electric field at the dielectric interface has a much higher amplitude in the slot region, which is shown in Figure 2.4. In Figure 2.4, we can observe that the electric field amplitude at the boundary interface of the slot region is the highest compared to its neighboring regions.

The field in the slot region represents an evanescent field, which decays exponentially as one moves away from the slot boundary. Therefore the slot width has to be less than the decay length of the evanescent wave in order to have an opical mode transmitted through the slot region. Slot waveguides with slot widths of 50 nm and 101 nm have been analysed in [10, 17].

The main essence of the slot waveguide is to confine the optical energy to a narrow low index material region. This would be advantageous in enhancing the externally applied electric field in the slot due to the narrow width of the slot region. Also, it utilizes the

material nonlinear properties of the low refractive index material inside the slot region. Photonic devices such as ring resonators have been realized using slot waveguides [17].

In this section, the operating principle for a slot waveguide has been explained, which will be utilized later in the design of a silicon electro-optic switch. The next section explains photonic crystals, whose inclusion in the design of the silicon electro-optic switch is the novelty of our research project.

2.4   Photonic crystals

2.4.1   Introduction

The advancement of electronics and telecommunication industry is driven by miniaturization and the goal to operate at high data speeds. Some of the issues of the miniaturization of electronic circuits as mentioned in [18] are high resistance and power dissipation. In order to overcome these issues, scientists are looking to use light instead of electrons as the fundamental unit to carry information. This is because light has advantages over electrons, such as a higher capacity to carry information.

Just as semiconductors are widely used in electronic circuits because one can control the electronic properties of such materials, scientists envisioned creating an analogous optical component, which controls the properties of photons in order to realize all-optical circuits. A new class of materials called photonic crystals have emerged; they are sometimes also referred to as semiconductors of photons. These materials are said to have the potential to enable optical integration [19]. Photonic crystals as defined in [19] "are artificially created materials in which the index of refraction varies periodically between high index region and low index region". The unique features of photonic crystals are discussed in the next subsection.

2.4.2 Important properties of photonic crytsals

PHOTONIC BANDGAP

One of the unique features of photonic crystals is the photonic bandgap. The property of the photonic bandgap is similar to the energy bandgap in semiconductors. Just as electrons are forbidden to have energy levels that correspond to the energy bandgap in a semiconductor, photons that have energy levels within the photonic bandgap range are not allowed to exist in the photonic crystal structure. The photonic bandgap property causes light of a frequency range that lies within the photonic bandgap to not propagate through the photonic crystal.

To explain the phenomenon of photonic bandgaps, consider a one-dimensional photonic crystal structure containing alternating layers of two different dielectric materials. When a wave is incident along the axis of periodicity of the photonic crystals, it undergoes partial reflections at each dielectric interface as it propagates through the photonic crystal. If the partial reflections undergo constructive interference, they form a total reflected way and the incident wave is reflected back. This case is shown in Figure 2.5.
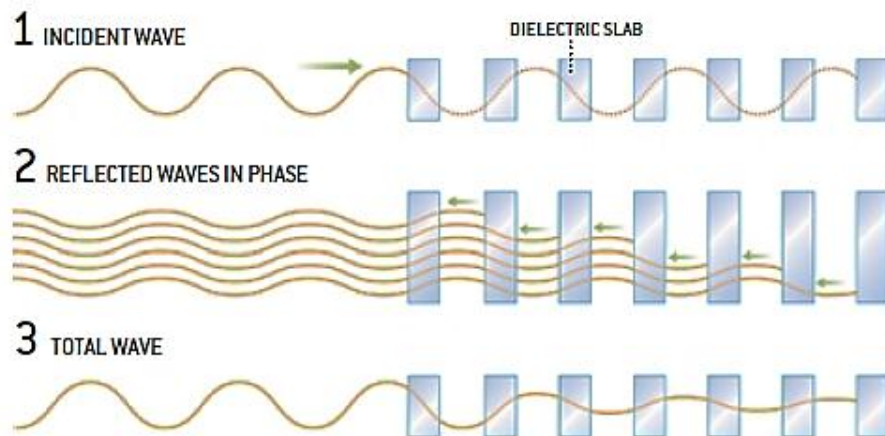
Figure 2.5 Illustration of an input wave whose wavelength lies inside the photonic bandgap travelling through the photonic crystal [20]

For wavelengths that do not lie within the photonic bandgap, the partial reflections at each dielectric interface are not in phase and undergo destructive interference, thus cancelling the reflected waves. Due to this, the incident waves propagate through the photonic crystal [21] .This case is shown in Figure 2.6. It should be noted that the periodic separation between the same dielectric material should be of the order of the wavelength of the incident light for the reflected waves to interfere.
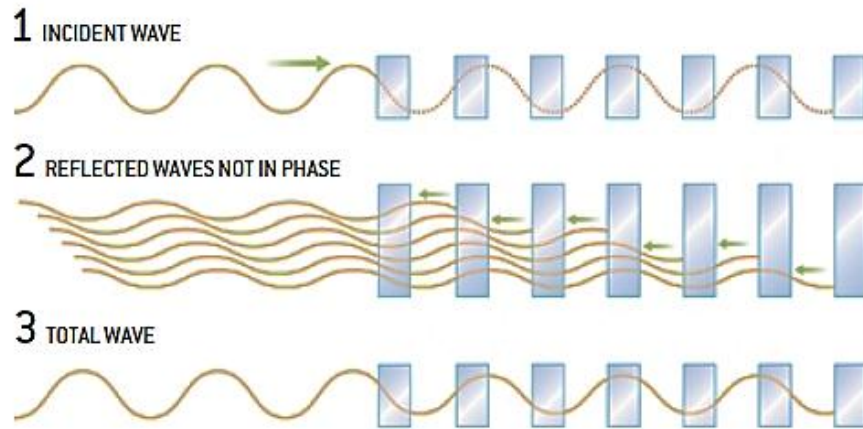
Figure 2.6 Illustration of an input wave whose wavelength lies outside the photonic bandgap travelling through the photonic crystal [20]

The explanation for the photonic bangap provided above is a traditional explanation pioneered by Lord Rayleigh to analyze a one-dimensional multilayer film [22].

A different approach to explain photonic bandgaps is the analysis of band structures. A band structure or band diagram for a medium is a plot that displays the allowed angular frequencies of the optical mode versus the angular wave numbers of the mode in the medium. It is obtained by solving the Maxwell's equations specific for the medium and obtaining a relationship between the wave vector and angular frequency for the optical mode (also known as dispersion relationship). Let us consider a multilayer film that corresponds to a one-dimensional photonic crystal as shown in the Figure 2.7.
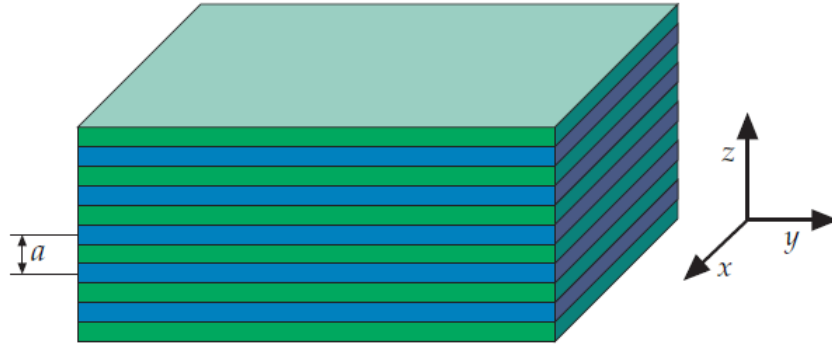
Figure 2.7 A Multilayer film [22]

A multilayer film is a one-dimensional photonic crystal because the refractive index changes periodically only in one direction, which is along the Z axis as shown in Figure 2.7. The periodic spacing between two layers of the same material is 'a'.
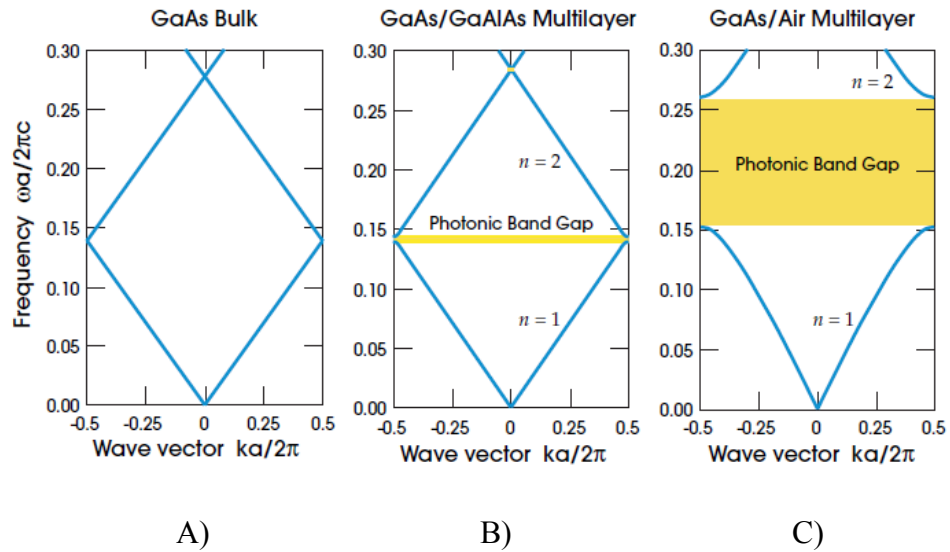
Figure 2.8 Photonic band diagrams for three different multilayer films [22]

The photonic band diagrams have been computed for three different multilayer films in [22] which are shown in Figure. 2.8. Figure 2.8 A) shows the band diagram when the multilayer film contains only GaAs (electric permittivity = 13). We can observe that the

modes correspond to the case of light line where $\omega(k) = \left(\frac{c_0}{\sqrt{\varepsilon}}\right) k$. Here, ω is the angular frequency of the mode, k is the wave vector of the mode in the medium, c_0 is the speed of light in vacuum and ε is the relative electric permittivity of the medium. In figure 2.8 B), the multilayer films are composed of GaAs and GaAlAs (electric permittivity = 12). In this case, we can observe there is a small frequency range where there is no optical mode. This frequency range corresponds to the photonic bandgap. In figure 2.8 C), where the multilayer films are composed of GaAs and air (electric permittivity = 1), we observe a larger photonic bandgap due to a higher dielectric constant contrast than the previous case. The physical reason for the photonic bandgap in the band diagram is that the lower frequency mode (n=1) is confined to the higher refractive index region and the higher frequency mode (n=2) is confined to the low refractive index region. Therefore a change in the refractive index (electric permittivity) causes the maxima and minima frequencies for the two modes (say n=1 and n=2) to be different at the band edge ($k = \pi/a$) and this results in a photonic bandgap, which is shown in figure 7 B) & 7 C). [22]

In summary, the photonic bandgap property for a one-dimensional photonic crystal has been explained. The theory explained using band structures can be extended for two- and three-dimensional photonic crystals. The next section focuses on the slow light property of photonic crystals.

SLOW LIGHT WAVEGUIDE

Commonly used optical switches rely on an interferometric design [19]. In such a design, the main principle used is the introduction of a relative phase shift between optical signals propagating through two different waveguides. The induced phase shift results in constructive (phase difference = 0) or destructive interference (phase difference = 180 degrees) when the two optical signals are combined. In this way, switching action is achieved.

One of the problems preventing large-scale optical integration is the relatively large size of high speed active elements. It has been reported that the smallest all-optical and electro-optic devices are of the order of millimeters with little potential to get smaller

[11]. The reason for this is that the refractive index changes induced in the material to electro-optic and nonlinear optical effects are very small, of the order of 10^{-3} [11]. So, the length of a material required to induce a phase shift of $\Delta\phi$ would be of the order of millimeters or more, and is obtained from the equation below:

$$L = \Delta\phi\lambda_{air}/\Delta n 2\pi \tag{2.2}$$

Here, L is the length of a material required to induce a phase shift of $\Delta\phi$ in an optical signal propagating through the material, λ_{air} is the wavelength of the optical signal in air and Δn is the refractive index change induced in the material.

Consider a waveguide in which the group velocity of the optical signal ($v_g = \frac{d\omega}{dk}$) is much smaller that the speed of light in air (c_0). Here, ω is the angular frequency and k is the angular wavenumber. Let the refractive index in the material of the waveguide be changed by a small amount Δn through an external stimulus, for example, an electric field. Now the change in the dispersion relationship $\omega(k)$, caused by a small Δn, can be approximated using perturbation theory [11] and it is obtained as:

$$\frac{\Delta\omega(k)}{\omega} \approx -\sigma\left(\frac{\Delta n}{n_L}\right) \tag{2.3}$$

Here, $\Delta\omega(k)$ is the shift in the photonic band mode for a fixed angular wave number k, ω is the angular frequency of the optical signal and σ is the fraction of the electric field energy inside the region where Δn is applied. The change in phase of the optical signal actually depends on change in the wave number ($\Delta k(\omega)$), which can be calculated from (2.3) as:

$$\Delta k(\omega) \approx -\frac{\omega\sigma}{v_g}\left(\frac{\Delta n}{n_L}\right) \tag{2.4}$$

We know that relative change in the phase shift induced in a waveguide of length L is given as:

$$\Delta\varphi = \Delta k(\omega)L \tag{2.5}$$

Substituting eq. (2.4) in eq. (2.5), we get the length of the waveguide required to induce a phase shift of $\Delta\varphi$ as:

$$L \approx -\left(\frac{\Delta\varphi}{2\pi}\right)\left(\frac{\lambda_{air}}{\sigma}\right)\left(\frac{v_g}{c}\right)\left(\frac{n}{\Delta n}\right) \tag{2.6}$$

From eq. (2.6), it can be concluded that a smaller v_g results in a shorter waveguide length to induce a required phase shift and thus the phase sensitivity of the waveguide is enhanced. In a waveguide made from a photonic crystal structure, the factor $\left(\frac{v_g}{c}\right)$ can be reduced as per the designer's requirement [19], and therefore the required length of the waveguide can be reduced. This is not achievable in a conventional waveguide where the factor $\left(\frac{v_g}{c}\right)$ is of the order of 1.
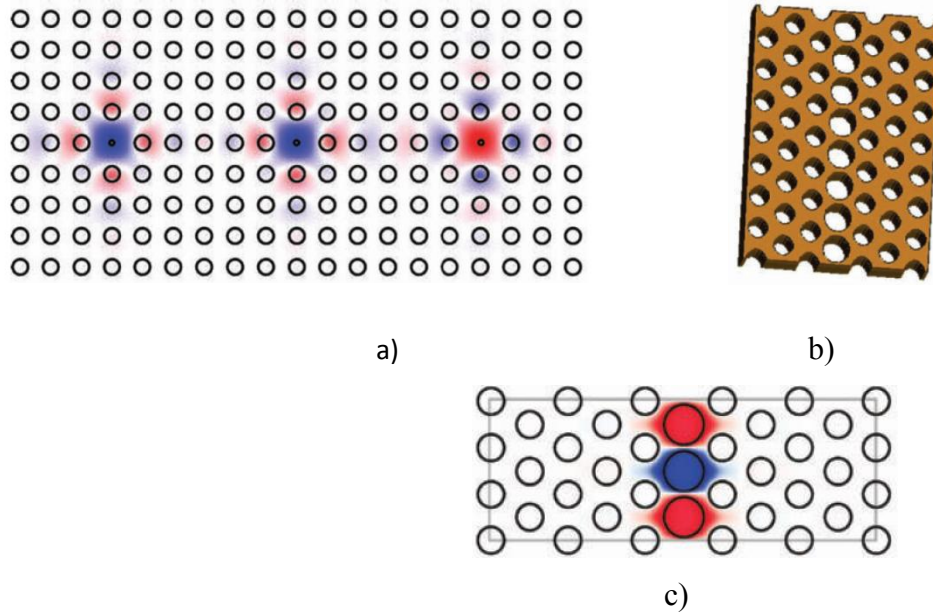
Figure 2.9 Coupled cavity waveguides [19]

Figure 2.9 a) shows high refractive index dielectric rods represented by circles that are surrounded by a low-refractive index medium. The defect in the PC structure introduced over here is a reduction of the radius of a dielectric rod and this defect is repeated after a periodic distance. By introducing this defect in the PC structure, light whose frequency lies in the photonic bandgap would be trapped inside the defect. But if these defects are repeated over a periodic distance, the light inside a defect would tunnel through to its neighbouring defect [19]. Thus, the line of defects in the PC structure acts as a waveguide.

Such types of photonic crystal waveguides are called coupled cavity waveguides (CCW) or coupled resonator oscillator waveguides (CROW) and the group velocity decreases exponentially as the separation between the defects increases [22]. Figure 2.9 b) shows a CCW with line defect in PC slab containing enlarged holes and the guided mode that propagates through this waveguide is shown Figure 2.9 c). The reduced group velocity of optical signal in the photonic crystal waveguide results in an enhanced $\Delta k(\omega)$, which is explained in the next paragraph.

The dispersion relationships for a photonic crystal waveguide (curved shape) and a conventional waveguide (straight line) have been calculated in [19] and are shown in Figure 2.10. Here a is the lattice constant for the photonic crystal waveguide, c is the speed of light in vacuum and Λ is the separation between the point defects. The effect of change in refractive index can be approximated to a parallel shift in the dispersion mode [19] which is shown by dotted lines for the photonic crystal waveguide and a conventional waveguide in Figure 2.10. For the same frequency shift of the dispersion mode in a conventional waveguide and a photonic crystal waveguide, the shift in the angular wavenumber k for a conventional waveguide is much smaller compared to that of a photonic crystal waveguide. This makes a photonic crystal waveguide more phase sensitive compared to a conventional high index contrast waveguide. Therefore for a given phase shift, the length of the photonic crystal waveguide required would be lesser compared to a conventional waveguide, and the reduced length of the waveguide can be calculated from eq. (2.6). There are different types of waveguides based on the photonic crystal structure used to achieve slow group velocities. Such waveguides are generally called slow light waveguides.
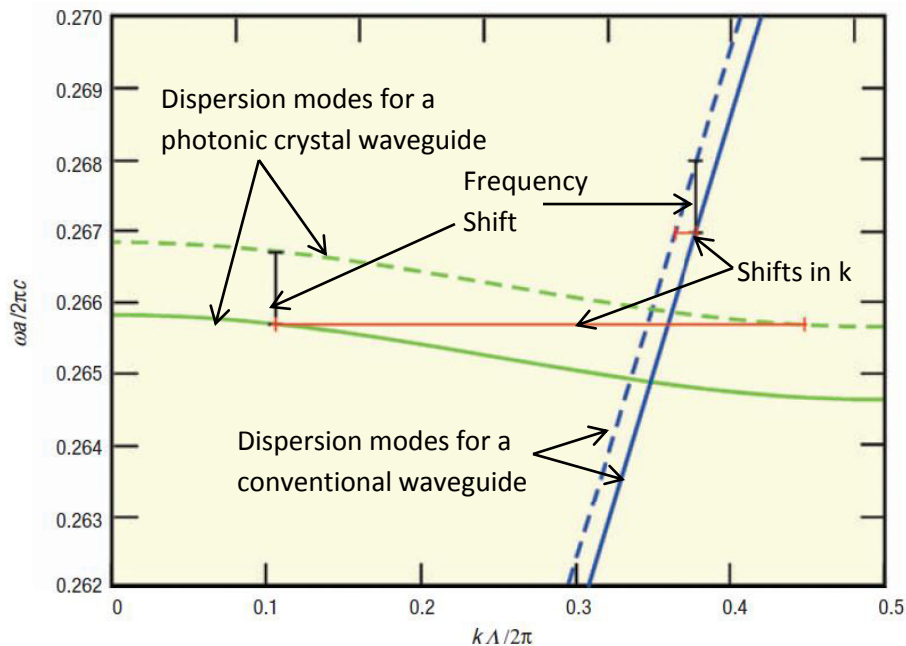

Figure 2.10 Plot comparing dispersion relationships between a photonic crystal waveguide and a conventional waveguide [19]

SLOW LIGHT APPLICATION FOR SWITCHING

A factor which is relevant for slow light applications is the slowdown factor S which is defined as "the ratio of the phase velocity over the group velocity, $S = v_\varphi/v_g$)" [23].

Most of the optical switching devices rely on relative phase change [23]. For example, a Mach-Zehnder interferometer requires a relative phase change of 180 degrees between the optical signals travelling through its two branches to achieve switching operation. Similarly, for a switch based on a ring resonator [8], the desired phase shift in the optical signal after one loop of propagation in the ring waveguide is 360 degrees. The phase shift of the optical signal is brought about by change in the angular wavenumber of the optical signal in the medium ($\Delta k(\omega)$), which is given by $\Delta k(\omega) = \Delta n\, k_0$. Here, Δn is the change in the refractive index, which can be induced by an external voltage source, and k_0 is the wavenumber of the optical signal in vacuum. The Δn that should be considered here is the change in the effective modal index of the material in the waveguide (Δn_{eff}) and not the material change in refractive index (Δn_{mat}) [23].

The effective refractive index is defined in [24] as:

$$n_{eff} = \beta/k_{air} \qquad (2.7)$$

Here, β is the propagation constant of the waveguide and k_{air} is the wavenumber of the mode in air. From (2.7), we can observe that a change in n_{eff} causes a change in the propagation constant of the waveguide which in turn results in a change in phase of the optical mode as it propagates through the waveguide.

In Figure 2.11, a mode (represented by the dark line) corresponds to a resonant condition of the waveguide which represented by a transmission peak on the right of Figure 2.11. A change in the material refractive index causes a parallel shift to the mode ($\Delta\omega(k)/\omega \approx \Delta n_{mat}/n$). Due to this resonant frequency of the waveguide shifts as per the new mode which shown by the dotted line in Figure 2.11.

The change experienced by the guided mode is different and is calculated from the change in the effective modal index (Δn_{eff}). The Δn_{eff} can be calculated from eq. (2.8) and (2.9) which are given below,

$$c = \omega/k \qquad (2.8)$$

$$c = c_0/n_{eff} \qquad (2.9)$$

We get,

$$\Delta n_{eff} = \left(\frac{c_0}{\omega}\right)(\Delta k(\omega)) \qquad (2.10)$$

Here, c is the phase velocity of the optical mode, ω is the angular frequency of the optical mode, k is the wavenumber of the mode in the waveguide and c_0 is the velocity of the optical signal in air. From Figure 2.11, we can observe that when one operates at a frequency in a region where the slope of the dispersion curve is small (the region which is almost parallel to the x axis, and is also called the slow light regime, ex.ω_2), the $\Delta k(\omega)$ and therefore Δn_{eff} is much greater than the case when one operates at a frequency (ex. ω_3) where the slope of the dispersion curve is steeper.
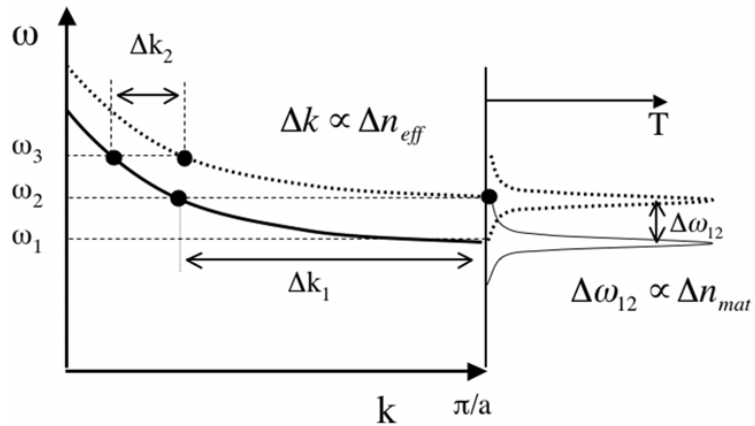

Figure 2.11 Effect of material change in refractive index and effective modal index [23]

As Δk varies as per the slope of the dispersion curve, it also varies as per the slowdown factor S ($\Delta k \propto 1/v_g \propto S$). Therefore,

$$\Delta k = \Delta n_{eff} k_0 \qquad (2.11)$$

$$\Delta k = S\Delta n_{mat} k_0 \qquad (2.12)$$

For conventional waveguides built from common materials S is of the order of 1 [19], but by using the concept of slow light that can be achieved using photonic crystals, one can extract a greater Δk and therefore make the waveguide more phase-sensitive.

In conclusion, the concept of slow light can be used to make the device more phase-sensitive, which would result in reducing the size of the device and /or the external energy required to operate the device. The next section discusses different slow light waveguide structures found in literature.

2.4.3 Slot and Slow Light Waveguides

Most applications of slow light photonic crystal waveguides use all-optical effects such as self-phase modulation, cross phase modulation, four wave mixing and the all-optical Kerr effect [13,11]. The application for our project is an electro-optic switch with the externally applied electric field being the controlling parameter. So the parameter to optimize would be the externally applied electric field and also to utilize the slow group velocity modes possible through photonic crystals. A waveguide structure that satisfies both these criteria is the combination of slot waveguides and photonic crystal structure. Slot waveguides as analysed in section 2.3 confine the optical signal to nanometer scale, and photonic crystals provide dispersion control. Examples of such structures are the slotted photonic crystal waveguides [25, 26] and the one-dimensional photonic crystals embedded into slot waveguide (1D PhoCSloW) [27].

The 1D PhoCSloW has been characterized at the telecommunication wavelength of 1.55 micrometers in [27], which is also the wavelength of operation for our proposed electro-optic switch. The structure considered is a rectangular slot waveguide with silicon as the high index material ($n_H = 3.5$) and silicon nanocrystals in silicon oxide as the low index material ($n_L = 1.65$) inside the slot.

In Figure 2.12, the Silicon layer thickness is $h = 300nm$ and the total waveguide width is $2W_H + W_S = 500nm$, with the slot width $W_S = 140nm$.
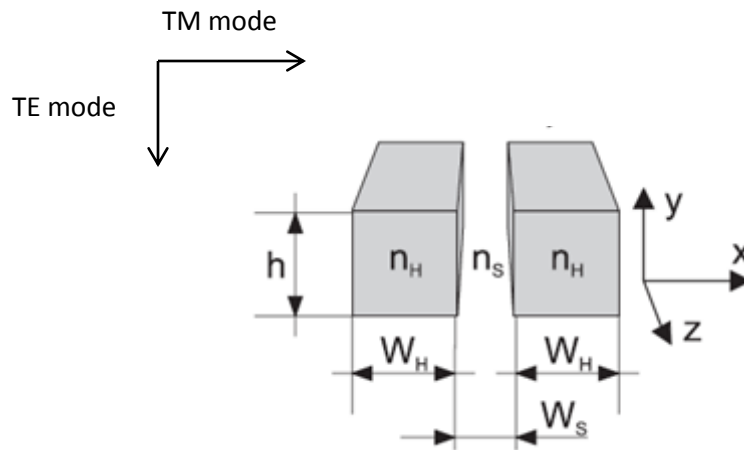

Figure 2.12 Basic geometry of a slot waveguide [27]

In the 1D PhoCSlow, the photonic crystal structure is introduced through air slits in the slot waveguide. Of the different types of configurations of the air slits that are analysed, the internal comb geometry is the preferred structure because it has a large photonic bandgap compared to the other configurations in [27].
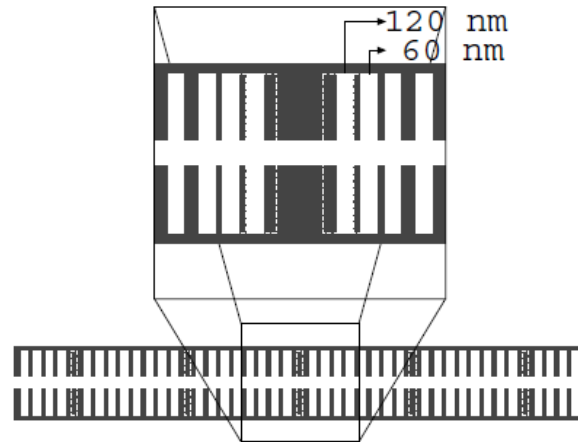
Figure 2.13 Geometry of a CROW device formed using the internal comb geometry [27]

The geometry of a coupled resonator oscillator waveguide (CROW) designed using the internal comb geometry of air slits is shown in Figure 2.13. The blown up image shows the optimizations used in [27] where the first air slit facing the cavity is shifted by 120 nm and the second air slit by 60 nm. The group velocity for the structure shown in Figure 2.13 was found to be $0.09c_0$ at an operating wavelength of 1.55 micrometers using FDTD simulation.[27] Here, c_0 is speed of light in vacuum.

In conclusion, a patterned slot waveguide can be used to make use of the advantages of the slow light effect instead of a conventional slot waveguide. The CROW device with the internal comb geometry discussed earlier can be directly integrated into a silicon waveguide, thereby reducing the size and complexity of the device.[27]

In the current chapter, the nanophotonic structures used in our research project — silicon nanocrystals, slot waveguides and photonic crystals — have been reviewed. A particular type of slow light photonic crystal waveguide, the 1D PhoCSloW, has been analyzed, which has potential to be applied to the Kerr switch in [8]. The next chapter discusses the electro-optic Kerr effect and how it would apply to the nanophotonic structures discussed in this chapter.

CHAPTER 3   ELECTRO-OPTIC KERR EFFECT

Electro-optic effects involve the change to the optical property of a medium when the medium is subjected to an electric field. This change to the optical properties is caused by atomic level changes in the material due to the applied electric field. Change in the optical property can refer to change in the refractive index of the medium. The change in the refractive index is utilized for implementing switches and modulators based on the electro-optic effect [1]. For an applied d.c electric field E, the refactive index varies only slightly and can be expanded using the Taylor's series. [1]

$$n(E) = n + a_1 E + \left(\frac{1}{2}\right) a_2 E^2 + \cdots \tag{3.1}$$

Here, $n = n(0)$, $a_1 = \left(\frac{dn}{dE}\right)$, $a_2 = \left(\frac{d^2n}{dE^2}\right)$; $at\ E = 0$ are the Taylor series coefficients and $n(E)$ is the refractive index of a material to the applied electric field. The relationship between the applied electric field and the change in the refractive index of the medium depends on the material of the medium. This relationship can either be linear or quadratic. The case when the relationship is linear is called the linear electro-optic effect or Pockels effect. The case when the change in the refractive index of the medium is proportional to the square of the applied external electric field is called the quadratic electro-optic effect or the Kerr effect [1]. An example of a medium that experiences the Pockels effect is Lithium Niobate. For a centrosymmetric medium, $n(E)$ is an even symmetric function and therefore $a_1 = 0$. Such a material is called a Kerr medium [1]. Silicon and silicon nanocrystals are examples of a Kerr medium.

A dielectric medium is characterised by its polarization density equation, which is given below [28]:

$$P(t) = \varepsilon_0 \left(\chi^{(1)}E(t) + \chi^{(2)} E^2(t) + \chi^{(3)} E^3(t) \ldots.\right) \tag{3.2}$$

Where $P(t)$ is the polarization density vector, $E(t)$ is the applied optical field, ε_0 electric permittivity of free space, $\chi^{(1)}$ is the leniar material susceptibility, $\chi^{(2)}$ and $\chi^{(3)}$ are the

second and third order material nonlinear susceptibilities. Here it is assumed that the medium is lossless, dispersion less and repond instantaneously.

Optical crystals such as lithium niobate have a large second order nonlinearity and are therefore commonly used to implement electro-optic switches and modulators based on the linear electro-optic effect [1,8]. Due to issues such as material compatibility with silicon, which is widely used in the electronics and telecommunication industry, the use of devices based on linear electro-optic materials has not become widespread [8]. For the semiconductor silicon which is a Kerr medium, $\chi^{(2)} = 0$ and the highest nonlinearity in the medium is $\chi^{(3)}$. The third order nonlinearity $\chi^{(3)}$ has been mostly used for all-optical effects such as four wave mixing and the optical Kerr effect. Instead of utilizing $\chi^{(3)}$ for all-optical effects, its electro-optic functionality is utilized to design a silicon-based electro-optic switch in [8]. Based on the review of various electro-optic effects relevant to silicon in [8], the Kerr effect is found the most suitable for the design of an ultrafast silicon-based electro-optic switch.

Section 3.1 aims to provide a explanation of the Kerr effect and its response for different silicon-based materials. Section 3.2 provides a Kerr effect analysis of slot waveguides and section 3.3 discusses losses that would have to be considered in the design of the silicon electro-optic switch.

3.1 Kerr Effect

The electro-optic Kerr effect requires an external stimulus, which is the externally applied electric field. So, this effect depends on an electric field and it is caused by the displacement of bound electrons in the material upon the application of the external electric field. The displacement of the bound electrons results in a nonlinear polarization in the medium. The generalized expression for the induced polarization in the medium is given by equation (3.2) which is repeated below,

$$P(t) = \varepsilon_0 \left(\chi^{(1)} E(t) + \chi^{(2)} E^2(t) + \chi^{(3)} E^3(t) \dots \right)$$

$$P(t) = P^{(1)}(t) + P^{(2)}(t) + P^{(3)}(t) \dots \tag{3.3}$$

In equation (3.3), $P^{(2)}(t)$ is the second order nonlinear polarization and $P^{(3)}(t)$ is the third order nonlinear polarization. From eq. (3.2) and (3.3), the third order nonlinear interaction is:

$$P^{(3)}(t) = \epsilon_0 \chi^{(3)} E^3(t) \tag{3.4}$$

The most general case for the applied field would consist of three different frequencies, which can be expressed as:

$$E(t) = E_1 e^{-i\omega_1 t} + E_2 e^{-i\omega_2 t} + E_3 e^{-i\omega_3 t} \tag{3.5}$$

Calculation of $E^3(t)$ will present different frequency components. When the expanded version of $E^3(t)$ is substituted in eq. (3.4), it is convenient to represent the third order nonlinear polarization as:

$$P^{(3)}(t) = \sum P(\omega_n) e^{-i\omega_n t} \tag{3.6}$$

where $P(\omega_n)$ is the complex amplitude of the nth frequency component of the third order nonlinear polarization.

The generalized expression for the third order nonlinear polarization for the frequency component $(\omega_1 + \omega_2 + \omega_3)$ using eq. (3.4) and (3.5) is as obtained [28],

$$P_i(\omega_1 + \omega_2 + \omega_3) = 3\epsilon_0 \sum_{jkl} \chi^{(3)}_{ijkl} (\omega_1 + \omega_2 + \omega_3, \omega_1, \omega_2, \omega_3) \times E_j(\omega_1) E_k(\omega_2) E_l(\omega_3) \tag{3.7}$$

In the above equation, $\chi^{(3)}_{ijkl} (\omega_1 + \omega_2 + \omega_3, \omega_1, \omega_2, \omega_3)$ represents the third order nonlinear susceptibility tensor and $ijkl$ refers to the cartesian components of the fields.

Let $\omega_1 = \omega$ represent an optical field and $\omega_2 = \omega_3 = 0$ represent the externally applied D.C electric field. Then eq.(3.7) reduces to:

$$P_i(\omega) = 3\epsilon_0 \sum_{jkl} \chi^{(3)}_{ijkl} (\omega; \omega, 0, 0) \times E_j(\omega) E_k(0) E_l(0) \tag{3.8}$$

The above equation describes the quadratic electro-optic Kerr effect (pure Kerr effect), where the propagation of light is controlled by the square of the applied dc electric field [29].

From eq.(3.7), we can observe that the third order nonlinear suceptibility of a material($\chi^{(3)}$) is frequency dependent or dispersive. But if one operates at a frequency that is far away from the material's resonant frequency , $\chi^{(3)}$ can be assumed to be dispersionless [8].

The nonresonant third order nonlinearity is present in all materials, but is not large (typical value around $\chi^{(3)} \sim 10^{-22}\ m^2/V^2$)[28] .This nonlinearity is important because of its instantaneous response time and hence could be used for an ultrafast switching application. The characteristic response time of the pure Kerr effect is the time taken to displace the electron cloud around a nucleus due to the applied electric field. This response time is estimated to be of the order of 10^{-16}seconds.[28]

The nonlinear polarization described by eq. (3.8) causes a change in the dielectric constant and therefore results in a change of the refractive index of the material.[8,29]. This change in the refractive index of the material (Δn) is given as [30]:

$$\Delta n = (3\chi^{(3)}/8n_L)E_{ext}^2 \qquad\qquad (3.9)$$

Here, $\chi^{(3)}$ is the third order nonlinear material susceptibility, n_L is the linear refractive index of the material and E_{ext} is the externally applied electric field.

The $\chi^{(3)}$ for materials relevant to our design of the electro-optic switch has been analysed and compared in Table 1 of Chapter 2. For device applications, a $\Delta n \geq 10^{-4}$ is desired [8].

Table 2 Comparison of induced change in refractive index for different materials

Material	Δn
Silica glass	5.68×10^{-9}
Bulk Silicon	3.21×10^{-6}
Silicon nanocrystals in silica	4.41×10^{-5}

For an externally applied electric field of $10\ V/\mu m$, Table 2 gives a comparison for the refractive index change in silica glass, bulk silicon and for silicon nanocrystals embedded in silica. Here, Δn is calculated using eq.(3.9). We can observe that there is at least an order of magnitude improvement in Δn for the material silicon nanocrystals embedded in silica.

The current section provided a theoretical description of the electro-optic Kerr effect. The next section analyses the application of the Kerr effect for the preferred slot waveguides.

3.2 Kerr effect analysis for Slot waveguides

As explained in Chapter 2, slot waveguides are the preferred waveguide structure for the design of the electro-optic switch. A schematic of the cross sectional view of a horizontal silicon slot waveguide with silicon nanocrystal material in the slot is shown in Figure 3.1 [31]. In Figure 3.1, we can observe that the slot layer of width t_s is filled with the material silicon nanocrystal (Si-nc). The amorphous silicon (a-Si) and crystalline silicon (c-Si) layers sorrounding the the slot region have thicknesses of t_1 and t_2 respectively. The whole slot waveguide is placed in layers of silicon dioxide of thickness t_3 and t_4.
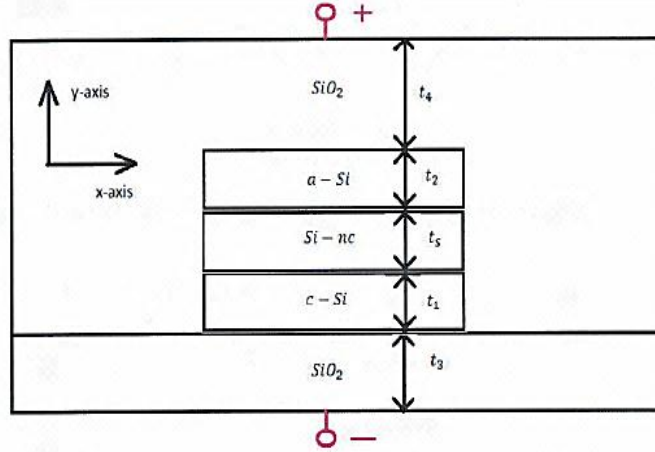
Figure 3.1 Cross sectional view of a biased slot waveguide [31]

To get an understanding of the practical functionality in terms of phase change of the optical signal propagating through the slot waveguide, we need to consider a slot waveguide of infinite width and with the thickness of the layers small enough so that the electric field within the slot can be assumed to be constant. This is shown in Figure 3.2.
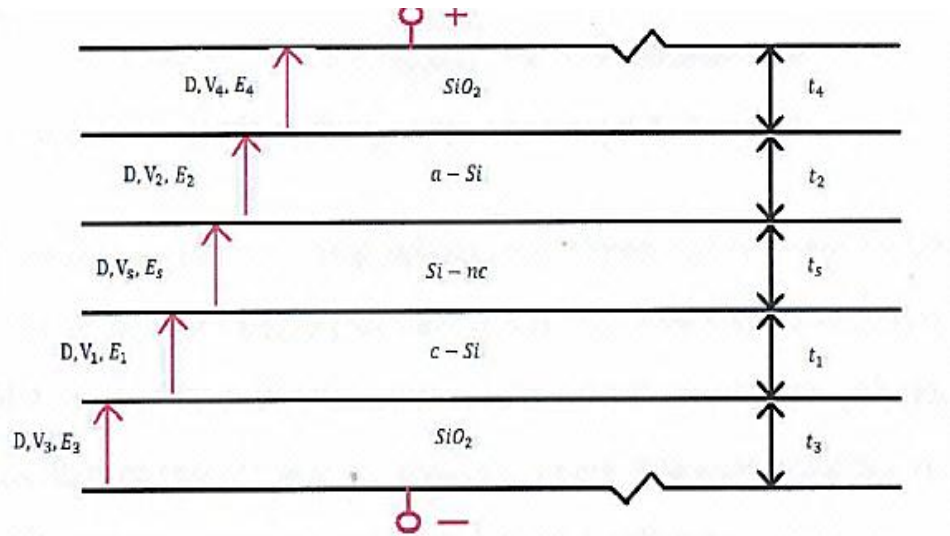
Figure 3.2 Schematic of a simplified horizontal slot waveguide with infinite width [31]

From Maxwell's boundary matching conditions, the electric fields within the layers can be expressed as:

$$E_1 n_{Si}^2 = E_s n_{Si-nc}^2 = E_2 n_{Si}^2 = E_4 n_{SiO_2}^2 = E_3 n_{SiO_2}^2 \qquad (3.10)$$

Here, E_1, E_2, E_3, E_4, E_s are the electric fields within the different layers shown in Figure 3.2, and n_{Si}, n_{Si-nc}, n_{SiO_2} are the refractive indices of the materials of the layers shown in Figure 3.2.

Let V_{ext} be the applied external voltage. Then, by Kirchhoff's voltage law, we have:

$$V_{ext} = V_1 + V_2 + V_3 + V_4 + V_s \qquad (3.11)$$

Here, V_1, V_2, V_3, V_4, V_s are voltages across the different layers in the slot waveguide as shown in figure 3.2. Using eq. (3.10) and eq. (3.11), we get the electric field inside the slot waveguide as:

$$E_s = V_{ext} / [\left(\frac{n_{Si-nc}}{n_{Si}}\right)^2 (t_1 + t_2) + \left(\frac{n_{Si-nc}}{n_{SiO_2}}\right)^2 (t_3 + t_4) + t_s] \qquad (3.12)$$

From eq. (3.12), it is clear that reducing the slot thickness is going to result in an increase of the electric field inside the slot with other parameters being the same. An increased E_s would result in a greater refractive index change due to the electro-optic Kerr effect.

From [30], the refractive index change due to the applied d.c electric field in the slot region ($E_{ext} = 2E_s$) can be written as:

$$\Delta n = \left(\frac{3\chi^{(3)}}{2n_L}\right) E_s^2 \qquad (3.13)$$

The $\chi^{(3)}$ of a material is related to the more well-known material constant, which is the Kerr coefficient or the nonlinear refractive index of a material (n_2) through the relationship [32] :

$$n_2 = \left(\frac{3}{4}\right)\left(\frac{\chi^{(3)}}{c n_L^2 \varepsilon_0}\right) \qquad (3.14)$$

In the above equation, ε_0 is the electric permittivity of free space and c is the speed of light in vacuum. Using eq. (3.14) in eq. (3.13), we get:

$$\Delta n = 2n_L c \varepsilon_0 n_2 E_s^2 \qquad (3.15)$$

For $E_s = 10V/\mu m$ the $\Delta n = 1.806 \times 10^{-4}$ for silicon nanocrystal material.

Using the concept of slow light explained chapter 2, we can write the change in the wave number of the optical mode (Δk) as it propagates along the slow light waveguide as:

$$\Delta k = Sk_0 \Delta n_{mat} = S(2\omega\varepsilon_0 n_L n_2 E_s^2) \tag{3.16}$$

Here, S is the slowdown factor of the waveguide.

So, the phase shift experienced by an optical signal as it propagates along a waveguide of length L to which an external electric field is applied is generally represented as:

$$\Delta\phi = \Delta kL \tag{3.17}$$

Using eq. (3.16) in eq. (3.17) we have:

$$\Delta\phi = 2S\omega\varepsilon_0 n_L n_2 E_s^2 L \tag{3.18}$$

From eq. (3.18), we can observe that the slow light effect has made the slot waveguide structure with photonic crystal more phase sensitive than a conventional slot waveguide due to the slowdown factor S which is greater than one. Equation (3.18) is a new equation specific for the electro-optic Kerr effect which includes the concept of slow light.

In conclusion, the application of the electro-optic Kerr effect has been analyzed for a slot waveguide. The induced refractive index change for silicon nanocrystals has been calculated. Also, the effect of slow light due to the inclusion of photonic crystals has been discussed with respect to phase sensitivity of the waveguide and a new expression has been derived for this case. The next section describes factors that account for losses in the operation of a silicon electro-optic switch.

3.3 Loss Analysis

One needs to consider optically induced losses such a linear absorption losses and nonlinear absorption losses for practical importance. This is because linear absorption can

lead to localized heating and cracking in the material [28]. Nonlinear absorption, such as the two photon absorption (TPA) process, would induce a refractive index change that can dominate over the refractive index change due to the electro-optic Kerr effect. This would result in slower operation speeds as the refractive index change through TPA is caused by free carriers [7].

Based on the experimental results in [12], silicon nanocrystals have almost negligible linear absorption at the wavelength of 1.55 micrometers. As a result, losses due to linear absorption can be neglected in the system. TPA is process where a bound electron in the valence band acquires sufficient energy from two incident photons to jump to the conduction band [28]. Two photon absorption is a third order nonlinear process that depends on the third order nonlinear susceptibility of a material ($\chi^{(3)}$). The TPA parameter of a material corresponds to the imaginary part of $\chi^{(3)}$. The TPA process can be prevented by keeping the operating wavelength below the half energy bandgap of the material [28, 8]. Also, as the silicon nanocrystal's diameter is reduced to the order of 3 nm or below, the bandgap of the material, and therefore the half bandgap energy of the material, is increased due to quantum confinement [33]. Based on the results obtained in [33], the operating wavelength of 1.55 micrometers (0.8 eV) is less than the half bandgap energy (0.93 eV for 3 nm diameter silicon nanocrystals) of the silicon nanocrystals material.

A drawback of the slow light effect is that the material's nonlinear loss parameter is enhanced by S^2 [13]. Here, S is the slowdown factor for the waveguide used. Based on the practical assumption in [30], the electric field due to the optical signal is much smaller than the externally applied electric field. Hence, all-optical effects, such as two photon absorption can be neglected, and the externally applied electric field can be made the dominating control parameter. It was also our objective to design a silicon electro-optic switch with external electric field as the device controlling parameter. Designing dispersion engineered structure, such as a coupled resonator oscillator waveguide suggested in [13] for achieving favourable loss dependence, is a possible topic of future work.

This chapter analyzed the electro-optic Kerr effect theoretically as well as its application for different materials such as silica glass, bulk silicon and silicon nanocrystals. The application of the Kerr effect for slot waveguides has also been presented and the loss factors that could decrease the efficiency of the electro-optic switch have been discussed. The next chapter provides the design considerations and simulation results for the silicon electro-optic switch.

CHAPTER 4   THE PROPOSED ELECTRO-OPTIC KERR SWITCH

A resonator cavity, such a Fabry Perot resonator or a ring resonator, has the ability to capture weak nonlinear interactions in the form of change in the transmitted output from the resonator due to its sensitivity to refractive index change [8]. This change in the transmitted output can be used to design modulators and switches [8,34]. A ring resonator is chosen for the design of our silicon-electro optic switch because it offers low operating voltage of the order of 1 V, and it has been experimentally analysed for a silicon electro-optic modulator [34]. A schematic of a single ring resonator is shown in Figure 4.1.

Output
optical
signal

Straight waveguide

Ring waveguide

Input
optical
signal
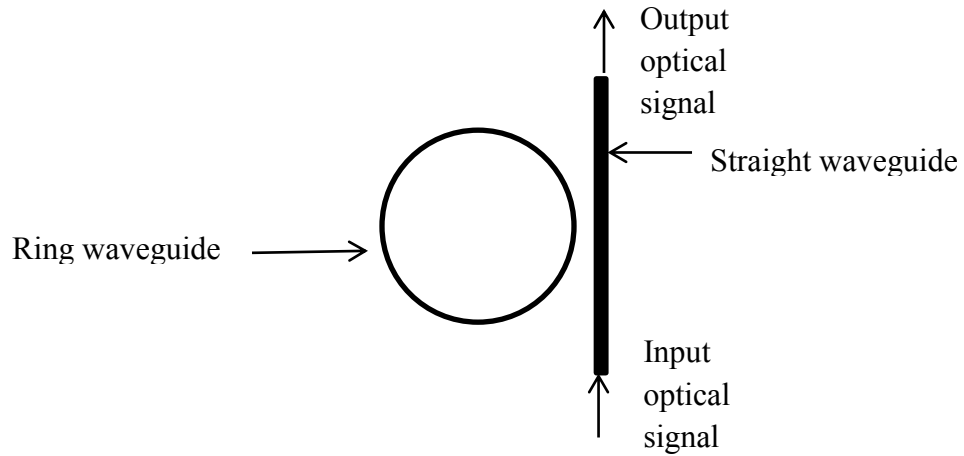
Figure 4.1 Schematic of a
single ring resonator

The principle of operation of a ring resonator is that when the input wavelength through the straight waveguide corresponds to a resonant wavelength of a ring resonator, then the input optical signal gets coupled to the ring waveguide because it is very close to the straight waveguide. This would lead to a reduction in the transmitted output power through the straight waveguide. The resonant wavelength of the ring resonator can be changed by changing the refractive index of the material inside the ring resonator. This can be done through an externally applied electric field because of the electro-optic Kerr

effect. Thus, this configuration can be used for optical switching through electric field control.

The normalized transmission spectra equation for single ring resonator is given in [35, 36].

$$T = (a_R{}^2 + t^2 - 2a_R t(\cos\theta))/(1 + (a_R t)^2 - 2a_R t(\cos\theta)) \tag{4.1}$$

Here, T is the transmission through the straight waveguide, $a_R = e^{-\alpha L}$ with α as the amplitude attenuation coefficient to account for losses due to bending and scattering in the ring waveguide, t is the straight through coefficient, and θ is the phase shift experienced by the optical signal after it completes one round trip of the ring waveguide. The expression to calculate θ is given by:

$$\theta = 2\pi n_{eff}\left(\frac{L}{\lambda_{air}}\right) \tag{4.2}$$

Here, n_{eff} is the effective modal index of the ring waveguide, L is the circumference of the ring waveguide and λ_{air} is the wavelength of the optical signal in air. At resonance $\theta = 2\pi m$ where m is an integer.

4.1 Optical structure

The same ring resonator structure employed in [34] is considered for the design of our silicon electro-optic switch. For the actual ring waveguide, the slot waveguide [8] and the slow light waveguide (1 D PhoCSloW) discussed in chapter 2 are analysed here. The horizontal configuration of the slot waveguide is proposed here. In this configuration the slot width can be reduced to well below 100nm, with slot widths of 50nm being fabricated [7]. The schematic of a horizontal slot waveguide is shown in Figure 4.2.
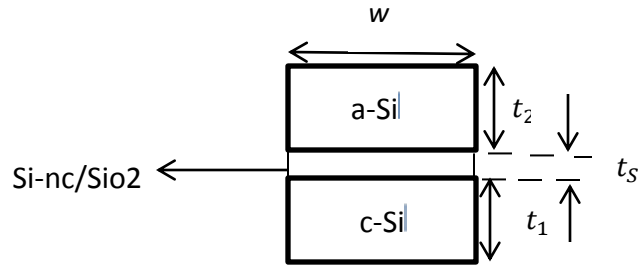
Figure 4.2 Schematic of the cross section of a horizontal slot waveguide [7]

In Figure 4.2 the waveguide width is w. The lower and upper strips of the slot waveguide are made of crystalline (c) and amorphous (a) silicon with thicknesses t_1 and t_2 respectively. The structure for a single ring resonator using a slot waveguide is shown in Figure 4.3.
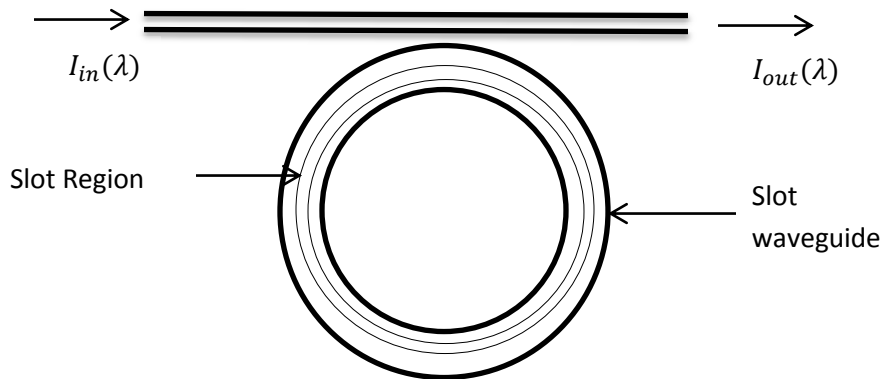
Figure 4.3 Schematic of a single ring resonator with a slot waveguide

The feasibility of an electro-optic Kerr effect switch can be estimated using the same ring resonator described in [34]. In the optimized horizontal structure for the slot waveguide considered in [8], the slot width is 100 nm and the effective refractive index for silicon nanocrystals in the fundamental mode is 2.06. The ring resonator described in [34] has a diameter of 12 micrometers, free spectral range (FSR) of 15 nm and 3 dB bandwidth or the full width at half maximum (FWHM) at resonance as 0.04 nm. In order to get an estimate on the feasibility of the Electro-Optic Kerr switch, the bending and scattering loss in the ring waveguide is approximated to be 6 dB/cm which is close to 6.8 dB/cm for

the ring waveguide of radius 10 micrometers [37]. The amplitude attenuation coefficient due to bending and scattering (α) is 69.14/m. The parameter (a_R) in eq. (4.1) for a ring waveguide length of 12π micrometers is 0.99739. The normalized transmission at resonance (P_{res}) from eq. (4.1) is,

$$P_{res} = \left(\frac{a_R - t}{1 - a_R t}\right)^2 \tag{4.3}$$

As $P_{res} = -15\ dB$ for the ring resonator considered in [34], the corresponding straight through coefficient (t) for the calculated a_R is, 0.99817. Using the parameters calculated, the transmission spectra for the ring resonator considered can be plotted using eq. (4.1) and this is shown in Figure 4.4.
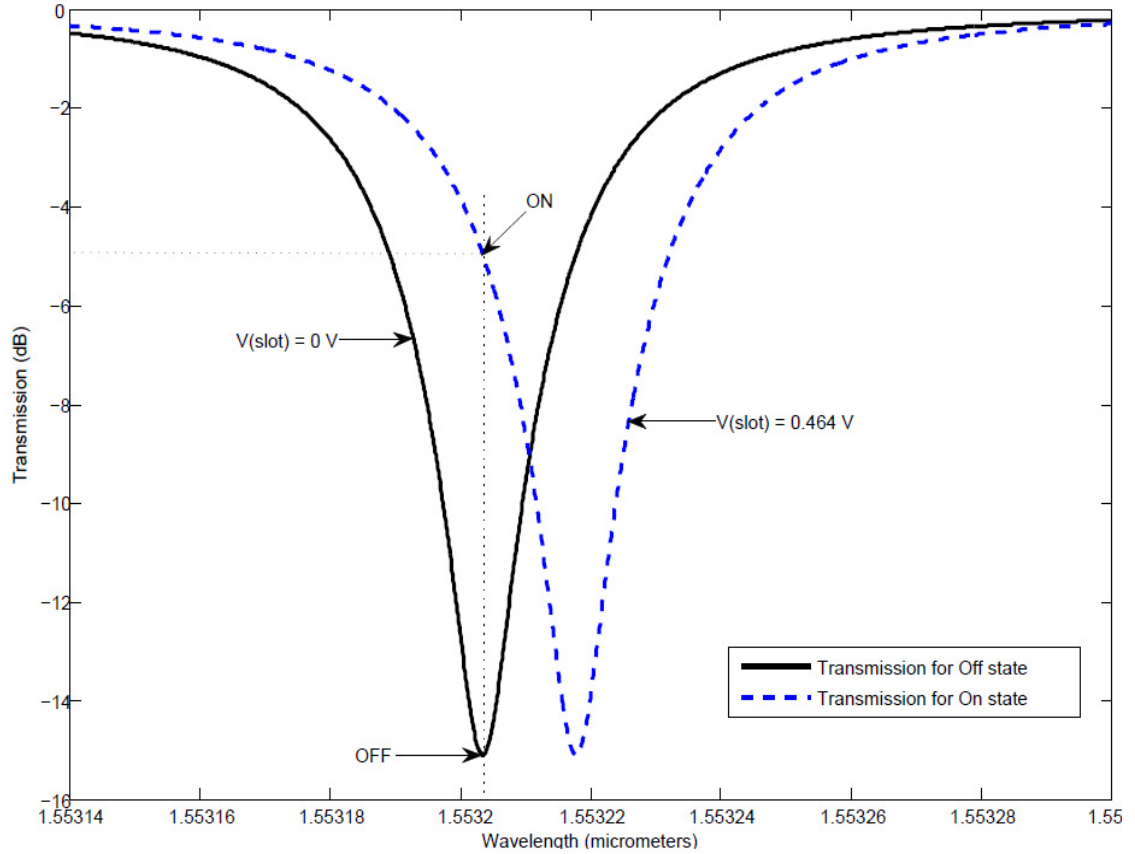

Figure 4.4 Transmission spectra of the electro-optic Kerr switch for $\Delta n_{eff} = 0$ (Off state) and $\Delta n_{eff} = 1.9 \times 10^{-5}$ (On state).

Figure 4.4 shows the transmission characteristics for zero change in refractive index (Off state of the switch) and for a required 10 dB extinction ratio at the operating wavelength (On state of the switch). The obtained 10 dB extinction ratio requires an effective index change of $\Delta n_{eff} = 1.9 \times 10^{-5}$ [8]. The approximate change in the material refractive index inside the slot region (Δn_{slot}) required to achieve the desired Δn_{eff} is, 3.8×10^{-5} [8]. For $\Delta n_{slot} = 3.8 \times 10^{-5}$, the voltage required across the slot region V (slot) is 0.464 V for a 100 nm wide slot. As calculated in Table 2, change in the refractive index for the material silicon nanocrystals in silica is 4.41×10^{-5} for an externally applied electric field of 1V/100 nm, which is greater than the required Δn_{slot}. Therefore the required 10 dB extinction ratio for switching is feasible through an available refractive index change in silicon nanocrystals. Also it was noted that considering higher bending losses in the ring waveguide such as 7 dB/cm or 7.5 dB/cm leads to a small reduction in the extinction ratio for the switch for the same operating conditions. The extinction ratio for the switch is reduced to around 9.5 dB which is reasonable.

THE PROPOSED STRUCTURE

Using a slow light waveguide such as the 1D PhoCSloW suggested in Chapter 2, one can reduce the externally applied electric field in order to achieve the same extinction ratio. This is because for a slow light waveguide operating in the slow mode, the change in the effective index is scaled by the slowdown factor (S) on applying an external electric field. For the structure of the ring resonator with the slow light waveguide, the slot waveguide in the ring resonator in Figure 4.3 can be replaced by a circular version of the coupled resonator oscillator waveguide shown in Figure 2.13.

The change in the resonant wavelength for the fundamental mode is,

$$\Delta \lambda_{res} = 2\pi R \Delta n_{eff} \qquad (4.3)$$

Here, $\Delta\lambda_{res}$ is the change in the resonant wavelength of the ring resonator, R is the radius of the ring resonator and Δn_{eff} is the change in the effective modal refractive index of the waveguide.

Let us consider the case when the ring resonator waveguide is replaced by a slow light waveguide. From eq. (2.12) we know that for a slow light waveguide $\Delta n_{eff} = S\Delta n_{mat}$, where S is the slowdown factor and Δn_{mat} is the material change in refractive index. Substituting eq. (2.12) in eq. (4.3) we have,

$$\Delta\lambda_{res} = 2\pi R S \Delta n_{mat} \tag{4.4}$$

Using eq. (3.9) for Δn_{mat} due to the electro-optic Kerr effect, the externally applied electric field is:

$$E^2 = 4\Delta\lambda_{res} n_L /(3\pi S\chi^{(3)} R) \tag{4.5}$$

Here, E is the applied d.c electric field in the active material of the ring waveguide and n_L is the linear refractive index of the material. Equation (4.5) is a new expression specific for the electro-optic Kerr effect with the application of the concept of slow light.

In comparison to a conventional ring resonator, we would have:

$$E_{new} = E_{old}/\sqrt{S} \tag{4.6}$$

Here, E_{old} is the applied d.c electric field for a conventional ring resonator and E_{new} is the applied d.c electric field for a ring resonator with a slow light waveguide. The reduction in the d.c electric field can be estimated by the example considered below.

For $S = 10/n_{eff}$, which is reported for 1 D PhoCSloW structure at a wavelength of 1.55 micrometers, if $E_{old} = 10V/\mu m$ then $E_{new} \cong 4.4\frac{V}{\mu m}$ assuming that n_{eff} for silicon nanocrystals in the structure considered is approximately 2. Hence, the required external electric field, and therefore the applied external voltage can be reduced. Thus the same extinction ratio in Figure 4.2 can be achieved using a smaller external electric field by employing a slow light waveguide.

The ring resonator size can be reduced using a slow light waveguide. From eq. (4.5) we can observe that the desired extinction ratio can be achieved by operating with the same external electric field and reducing the radius of the ring resonator. This would result in a smaller device size, which is useful for large scale integration. However, the losses due to bending and scattering would be increased due to the smaller ring radius so one would have to do a trade-off analysis between the ring radius and losses.

4.2 Challenges

Some of the challenges as noted in [8] for the design of the electro-optic Kerr effect switch are as follows,

1. The true electric Kerr constant of silicon nanocrystals at an operating wavelength of 1.55 micrometers needs to be found out experimentally so that it can be correctly used to calculate the material change in refractive index.
2. A figure of merit that takes into account the structural details applicable to the electro-optic Kerr effect needs to be established.
3. Analysis of loss due to nonlinear absorption in silicon nanocrystals and other losses due to free carrier effect in silicon needs to be carried out for a practical implementation of the electro-optic Kerr switch.
4. Analysis of electrical parasitics that could potentially degrade the performance of the high speed electro-optic switch needs to be carried out.
5. A comparative characterization of the ring and Fabry-Perot micro-resonators in terms of achievable parameters for an electro-optic Kerr effect device needs to be done.

In conclusion, the basics of a single ring resonator have been reviewed. Transmission spectra for the Kerr switch in [8] has been simulated and its feasibility using the material silicon nanocrystals in silica is presented. The internal comb structure of the 1DPhoCSloW is proposed as the slow light waveguide for the ring resonator in the silicon electro-optic switch. A preliminary analysis for effect of inclusion of a slow light waveguide in the ring resonator structure for the electro-optic Kerr effect switch has been

presented. The challenges faced in the design of the electro-optic Kerr switch are also discussed.

CHAPTER 5   CONCLUSION

This chapter summarizes the main contributions in this thesis and lists future steps to build upon the work carried out in this thesis.

5.1 Summary

The main contribution of this thesis is the inclusion of photonic crystals, which are nanophotonic structures, in the design of an ultrafast silicon electro-optic switch. It was theoretically shown that slow waveguides provide enhanced phase sensitivity compared to a conventional waveguide and therefore reduced the external electric field required to operate the switch. The enhanced phase sensitivity has been previously used for all-optical effects, but in this thesis it is utilized for the electro-optic Kerr effect. Different slow light waveguides, which are made up of photonic crystals, were analysed and the internal comb geometry of the 1D PhoCSloW is proposed for use in the ring resonator of the silicon electro-optic switch. The use of the slow light waveguide is expected to bring the following improvements for the silicon-electro optic switch:

1)   Reduce the switching energy required to operate the switch because the required external electric field is reduced.

2)   Reduce the radius of the ring resonator and thereby reduce the size of the switch

One has to consider the enhancement in the nonlinear absorption loss in slow light waveguides and also increase in scattering and bending losses due to reduction in the ring radius in the design of the silicon electro-optic switch.

In conclusion, the application and possible use of photonic crystals for the ultrafast silicon electro-optic switch proposed in [8] has been analysed. It was shown that the use of slow light waveguides has the potential to reduce the required externally applied electric field and the radius of the ring resonator. This is expected to reduce the switching energy and size of the electro-optic switch. The simulation used in this thesis was carried out using licensed Matlab software.

5.2 Future Work

For further development of the work carried out in this thesis, the following are some of the important future steps:

1) Formulation of a device figure of merit applicable to quadratic electro-optic Kerr effect devices. This would involve analysis of the device structure in terms of dimensions and also a nonlinear loss analysis for the electro-optic Kerr effect device.

2) Methods to eliminate polarization dependent losses in the silicon electro-optic switch. This would be especially useful for integrated optic applications where polarization maintaining fibers are used.

3) Calculation of the effective refractive index of silicon nanocrystals used in the proposed slow light waveguide in order to characterize the transmission spectra for the switch.

4) Calculation of the electrical parameters required to practically implement the designed ultrafast silicon electro-optic switch. This would give a practical measure for the achievable speed in the electro-optic Kerr effect switch.

REFERENCES

[1]   B E.A.Saleh and M.C Teich, Fundamentals of Photonics. New York: John Wiley & Sons, Inc., 1991.

[2]   R A. Soref and B R. Bennett, "Electrooptical effects in Silicon", IEEE Journal of   Quantum Electronics, vol. QE-23, no. 1, Jan. 1987, pp. 123-129

[3]   B.Jalali & S. Fathpour, "Silicon Photonics", Journal of Lightwave Technology,   vol. 24, no. 12, Dec. 2006, pp. 4600-4615.

[4]   P. N. Prasad, Nanophotonics, 1st ed., Canada: A John Wiley & Sons, Inc., 2004.

[5]   L. Novotny & B. Hecht, Principles of Nano-Optics, Cambridge, England: Cambridge United Press, 2008.

[6]   L.Liao et al., "40 Gbit/s silicon optical modulator for high speed applications", Electronic Letters, vol. 43, no. 22, Oct. 2007.

[7]   A. Martinez et al., "Ultrafast All-Optical Switching in a Silicon-Nanocrystal- Based Silicon Slot Waveguide at Telecom Wavelengths", Nano Letters, vol. 10, 2010, pp. 1506-1511.

[8]   M. Cada & J.Pistora, "Electro-Optic functionalities with Kerr Optical media", ISMOT, Prague, June 2011, pp. 445-453, Invited talk.

[9]   G.V. Prakash et al., "Nonlinear optical properties of silicon nanocrystals grown by plasma-enhanced chemical vapour deposition", Journal of Applied Physics, vol. 91, no. 7, Apr. 2002, pp. 4607- 4610.

[10]   V.R. Almeida et al. "Guiding and confining Light in void nanostructure", Optic   Letters, vol. 29, No. 11, Jun. 2004, pp. 1209-1211.

[11]   M. Soljacic et al., "Photonic Crystal slow-light enhancement of nonlinear phase sensitivity", Optical Society of America, vol. 19, no. 9, Sep. 2002, pp. 2052-2059

[12]   S. Hernandez et al., "Linear and nonlinear optical properties of Si nanocrystals in   SiO2 deposited by plasma enhanced chemical-vapour deposition", Journal of   Applied Physics vol. 103, no. 064309, Mar. 2008, pp. 064309-1 – 064309-6.

[13]   C. Monat et al., "Slow light enhanced nonlinear optics in periodic structures",   Journal of Optics, vol. 12, no. 104003, Sep. 2010, pp. 1-17.

[14]   M. Cada, private communication.

[15]   J.M. Ballesteros et al., "Nanocrystal size dependence of third order nonlinear   optical response of Cu:Al2O3 thin films", Applied Physics Letters, vol. 74, no.   19, May 1999, pp. 2791- 2793

[16]   M. H Nayfeh L. Mitas, V. Kumar (Ed.), Nanosilicon, Elsvier, 2008.

[17]   Q. Xu et al., "Experimental demonstration of guiding and confining light   in   nanometer-size   low-refractive-index   material",   Optics Letters, vol. 29, no. 14, Jul.   2004, pp. 1626-1628

[18]   J. D Joannopolous et al., "Photonic crystals: putting a new twist on light", Nature, vol. 386, Mar. 1997, pp. 143-149.

[19]   M. Soljacic & J. Joannopoulos, "Enhancement of nonlinear effects using photonic crystals", Nature Materials, vol. 3, Apr. 2004, pp. 211-219.

[20]   E. Yablonovitch, "Photonic Crystals: Semiconductors of light", Scientific American, Dec. 2001, pp-47-55

[21]   O. Takayama, "Numerical Analysis on Polymer and Metallo-Dielectric Photonic Crystals", MASc. thesis, Electrical & Computer   Engineering, Dalhousie University, Halifax, Nova Scotia, 2004.

[22]   J. D. Joannopolous et al., Photonic Crystals: Molding the flow of light, 2nd edition, Princeton NJ: Princeton University Press, 2008

[23]   T. F. Krauss, "Slow light in photonic crystal waveguides", Journal of Physics D: Applied Physics, vol. 40, 2007, pp. 2666-2670

[24]   K. J. Ebeling, Integrated Opto-electronics, 2nd edition, Berlin, Germany: Springer-Verlag, 1993

[25]   A. Di Falco et al., "Dispersion control and slow light in slotted photonic crystal waveguides", Applied Physics Letters, vol. 92, 2008, 083501-1 -- 083501-3

[26]   A. Di Falco et al., " Photonic crystal slotted slab waveguides ", Elsevier Photonics   and nanostructures- Fundamentals and Applications, vol. 6, 2008, pp. 38-41

[27]   F. Riboli et al., "Bandgap characterization and slow light effects in one dimensional photonic crystals based on silicon slot-waveguides", Optics Express, vol. 15, no. 19, Sep. 2007, pp. 11769- 11775

[28]   R W. Boyd, Nonlinear Optics, 3rd edition, Amsterdam: Elsevier, 2008

[29]   E.G. Sauter, Nonlinear Optics, New York: John Wiley & Sons, Inc., 1996

[30] M. Cada et al., "Electrically and optically controlled cross-polarized wave   conversion", Optics Express, vol. 16, no. 5, 2008, pp. 3083-3100

[31] M. Cada, "Kerr effect in slot waveguide with Si-nc", Research Report, Nanophotonic Technology Center, Valencia, Spain, 2008.

[32] J. Leuthold et al., "Nonlinear silicon photonics", Nature Photonics, vol. 4, Aug.   2010, pp. 535-544

[33] R. J Walters, "Silicon nanocrystals for Silicon Photonics", PhD thesis, California Institute of Technology, Pasadena, California, 2007

[34] Q. Xu et al., "Micrometer-scale silicon electro-optic modulator",   Nature letters, vol. 435, pp. 325-327

[35] R. Vafei, "Silicon on Insulator ring resonators", EECE 571u Course Project Report.

[36] D.G. Rabus, Integrated ring resonators: the compendium, Berlin: Springer, 2007.

[37] C.A. Barrios, "High-performance all-optical silicon microswitch", Electronics Letters, vol. 40, No. 14, Jul. 2004.